The paper was presented at the Eighth Meeting
"New Trends in Fatigue and Fracture" (NT2F8)
Ankaran, Slovenia, 23–24 October, 2008

Nabil Kazi Tani [1], Tawfik Tamine [1], Guy Pluvinage [2]

NUMERICAL EVALUATION OF THE STRAIN ENERGY RELEASE RATE WITH ORIENTATION AND POSITION OF A CRACK NEAR A BIMATERIAL INTERFACE

NUMERIČKA OCENA BRZINE OSLOBAĐANJA ENERGIJE DEFORMACIJE SA ORIJENTACIJOM I POLOŽAJEM PRSLINE BLIZU INTERFEJSA BIMATERIJALA

Originalni naučni rad / Original scientific paper
UDK /UDC: 539.42:519.673
Rad primljen / Paper received: 25.01.2009

Adresa autora / Author's address:
[1)] Laboratory LCGE, Faculty of Mechanical Engineering, University of Sciences and Technology of Oran, BP 1505 EL M'NAUER 31000 Oran, Algeria, Kazitani_nabil@yahoo.fr
[2)] Laboratoire de Fiabilité Mécanique ENIM, Metz, France pluvina@univ-metz.fr

Keywords
- bi-material
- interfacial crack
- mixed mode fracture
- stress intensity factor
- energy release rate
- finite element

Ključne reči
- bimaterijal
- prslina na interfejsu
- mešoviti oblik loma
- faktor intenziteta napona
- brzina oslobađanja energije
- konačni element

Abstract

The finite element method and fracture mechanics concept were used to study the interfacial fracture of bi-material structure. Effects of mechanical materials properties, position and orientation between crack and bimaterial interface are presented. Numerical results show that the energy release rate of the interfacial crack is influenced considerably by parameters of these effects. For several examples studied, a good agreement is obtained with different authors in term of normalised stress intensity factor and energy release rate.

Izvod

Metoda konačnih elemenata i koncept mehanike loma su korišćeni za proučavanje loma interfejsa strukture od bimaterijala. Izraženi su uticaji mehaničkih osobina materijala, položaja i orijentacije prsline u odnosu na interfejs bimaterijala. Numerički rezultati pokazuju da brzina oslobađanja energije prsline na interfejsu u značajnoj meri zavisi od parametara ovih uticaja. Za više proučavanih primera dobijena je dobra saglasnost rezultata različitih autora prikazanih preko normalizovanog faktora intenziteta napona i brzine oslobađanja energije.

INTRODUCTION

Many authors have studied cracks in complex media as nonhomogeneous materials. Recently, some researchers have been interested in the problems of the interfacial cracks in bimaterial plates. P.R. Marur and H.V. Tippur, /1/, have solved interfacial crack problems in bimaterial plates analytically by the development of stress field formulations into analytical series. Using the boundary element method (BEM), Yijun J. Liu and Nan Xu, /2/, have determined stress intensity factors for curved interfacial cracks. The same parameters have been expressed analytically by J.P Shi, /3/, using variational approach. In their paper, C. Bjerken and C. Persson, /4/, have used the crack closure integral method to determine complex formulation of stress intensity factors for cracks at the interface in bimaterial plates.

For cracks perpendicular to the interface, T.C.Wang and P. Stahle, /5/, have determined the stress field near the crack tip by using Muskhelishivili's potentials. Yilan and Hua, /6/, have calculated stress intensity factors from displacement equations near the crack tip for an edge crack perpendicular to the interface, where the position of crack tip is at the interface.

Using photoelasticity experimental techniques, A. Cirello and B. Zuccarello, /7/, have studied the effect of crack propagation perpendicular to the interface in nonhomogenous media which contains two dissimilar materials.

The aim of present study is to describe the effects of position and crack orientation with the presence of interfaces in bimaterial plates on the fracture parameters, especially the stress intensity factor K and energy release rate G.

The influence of crack length a and fracture mixed modes have been developed in this paper for cases of cracks parallel and perpendicular, and also inclined to the interface. The results obtained numerically have been compared to recent research works.

BASIC FORMULAE

Stress field for crack parallel to bimaterial interface

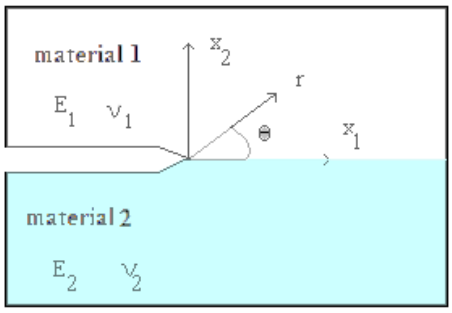

Figure 1. Crack geometry and coordinate system in bimaterial plate.
Slika 1. Geometrija prsline i koordinatni sistem bimaterijalne ploče

The complex form of the stress field near the crack tip for a crack at the interface can be expressed as follows, /8/:

$$\sigma_{\alpha\beta} = \frac{\Re e\left[Kr^{i\varepsilon}\right]}{\sqrt{2\pi r}}\Sigma^{I}_{\alpha\beta}(\theta,\varepsilon) + \frac{\Im m\left[Kr^{i\varepsilon}\right]}{\sqrt{2\pi r}}\Sigma^{II}_{\alpha\beta}(\theta,\varepsilon) \quad (1)$$

where (r, θ) are polar coordinates of the system and (α, β) are material indices 1 and 2.

The parameter, ε, that characterizes bimaterial specimen is defined by the equation:

$$\varepsilon = \frac{1}{2\pi}\ln\left(\frac{1-\beta_D}{1+\beta_D}\right) \quad (2)$$

with b_D, the Dundur's parameter, /9/, given as follows:

$$\beta_D = \frac{\mu_1/\mu_2(k_1-1)-(k_2-1)}{\mu_1/\mu_2(k_1+1)+(k_2+1)} \quad (3)$$

with $k_j = 3 - 4\nu_j$ in plane strain; $k_j = \dfrac{3-\nu_j}{1+\nu_j}$ in plane stress.

The complex stress intensity factor K is defined as:

$$K = K_1 + iK_2 = |K|e^{i\kappa} \quad (4)$$

where κ is the phase angle that depends on the bimaterial constant ε.

Functions $\Sigma^{I}_{\alpha\beta}(\theta,\varepsilon)$ and $\Sigma^{II}_{\alpha\beta}(\theta,\varepsilon)$ equal unity along the interface ahead of the crack tip for $\theta = 0$. For the case $\theta \neq 0$, the angular functions can be found in /10/.

For $\varepsilon = 0$, Eq. (1) is reduced to the expression for the stress field close to crack tip in a homogeneous material.

For $\theta = 0$, stresses σ_{22} and σ_{12} at the interface directly ahead of the tip are given by:

$$\sigma = \sigma_{22} + i\sigma_{12} = \frac{K_1 + iK_2}{\sqrt{2\pi r}}r^{i\varepsilon} \quad (5)$$

Associated crack surface displacements, δ_1 and δ_1, at a distance r behind the tip, $\theta = \pi$, are given by, /4/:

$$\delta = \delta_2 + i\delta_1 = \frac{8(K_1+iK_2)}{(1+2i\varepsilon)\cosh(\pi\varepsilon)}\sqrt{\frac{r}{2\pi}}\frac{r^{i\varepsilon}}{E^*} \quad (6)$$

with

$$\frac{1}{E^*} = \frac{1}{2}\left(\frac{1}{\bar{E}_1} + \frac{1}{\bar{E}_2}\right) \quad (7)$$

$\bar{E}_j = E_j/(1-\nu_j^2)$ in plane strain; $\bar{E}_j = E_j$ in plane stress; and $j = 1; 2$.

When the possibility of crack advance is considered, the energy release rate is often used as a measure of driving force. For an interfacial crack, Malyshev and Salganik, /11/, showed that the energy release rate, G, in terms of complex stress intensity factor, K, is:

$$G = \frac{|K|^2}{\cosh^2(\pi\varepsilon)E^*} \quad (8)$$

Stress field for the crack perpendicular to bimaterial interface

Consider the plane elastic problem as shown in Fig. 2, when a finite crack is perpendicular to the bimaterial interface. A Cartesian coordinate system Oxy is attached on the interface. The x axis is along the interface and the y axis is normal to the interface and coincides with the crack elongation direction, /5/.

Both materials are isotropic and homogeneous. Material I is occupied by the upper half plane S_1 and material II is occupied by the lower half plane S_2.

Stress and displacement in an elastic solid can be represented by two Muskhelishivili potentials:

$$\begin{aligned}&\sigma_x + \sigma_y = 4\Re e(\Phi(z))\\ &\sigma_y - i\tau_{xy} = \Phi(z) + \Omega(\bar{z}) + (z-\bar{z})\overline{\Phi'(z)}\\ &2\mu(u_x + iu_y) = \kappa\Phi(z) - \Omega(\bar{z}) - (z-\bar{z})\bar{\Phi}(z)\end{aligned} \quad (9)$$

Here $\Phi(z)$ and $\Omega(z)$ are complex potentials.

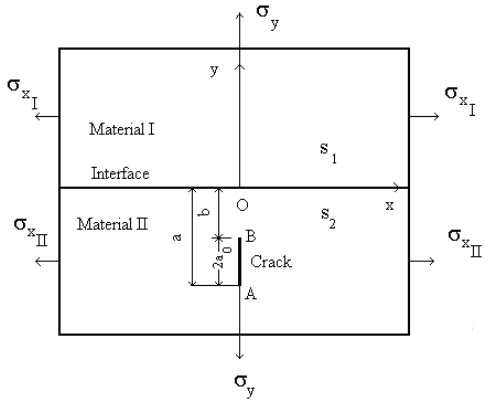

Figure 2. A finite crack perpendicular to a bimaterial interface.
Slika 2. Konačna prslina upravna na interfejs bimaterijala

The complex potentials for an edge dislocation at $Z = S$, in an infinite elastic solid can be expressed as follows:

$$\begin{aligned}&\Phi_0(z) = \frac{B}{z-s};\quad \Omega_0(z) = \frac{B}{z-s} + \bar{B}\frac{s-\bar{s}}{(z-s)^2}\\ &B = \frac{\mu}{\pi i(\kappa+1)}(b_x + ib_y)\end{aligned} \quad (10)$$

where b_x and b_y are x and y components of dislocation, $\kappa = 3 - 4\nu$ for plane strain, ν is Poisson's ratio, and μ is the shear modulus.

If the edge dislocation is embedded in material II, the complex potentials are (see Suo, /12/):

$$\Phi(z)=\begin{cases}(1+\Lambda_1)\Phi_0(z) & z=S_1\\ \Phi_0(z)+\Lambda_2\Omega_0(z) & z\in S_2\end{cases} \quad (11)$$

$$\Phi(z)=\begin{cases}\Phi_0(z)+\Lambda_1\Omega_0(z) & z=S_1\\ (1+\Lambda_2)\Phi_0(z) & z\in S_2\end{cases} \quad (12)$$

$$\Lambda_1=\frac{\alpha_D+\beta_D}{1-\beta_D} \qquad \Lambda_2=\frac{\alpha_D-\beta_D}{1+\beta_D} \quad (13)$$

where α_D and β_D are two Dundur's, /9/, parameters:

$$\alpha_D=\frac{(\kappa_2+1)/\mu_2-(\kappa_1+1)/\mu_1}{(\kappa_2+1)/\mu_2+(\kappa_1+1)/\mu_1}$$
$$\beta_D=\frac{(\kappa_2-1)/\mu_2-(\kappa_1-1)/\mu_1}{(\kappa_2+1)/\mu_2+(\kappa_1+1)/\mu_1} \quad (14)$$

The crack can be considered as a continuous distribution of dislocations. Hence for our problem, we have:

$$\Phi_0(z)=\frac{\mu_2}{\pi i(1+\kappa_2)}\int_a^b\frac{(bx+iby)}{z+it}dt \quad (15)$$

$$\Omega_0(z)=\frac{\mu_2}{\pi i(1+\kappa_2)}\int_a^b\frac{(bx+iby)}{z+it}dt+\frac{\mu_2}{\pi(1+\kappa_2)}\int_a^b\frac{t(bx-iby)}{(z+it)^2}dt$$

where a and b are distances from crack tips A and B to the interface, respectively.

Let us introduce a new complex variable z^* and a new function $\mathrm{I}(z^*)$, where $z^*=iz$,

$$\mathrm{I}(z^*)=\frac{1}{\pi}\int_a^b\frac{bx+iby}{z^*-1}dt \quad (16)$$

The function $\mathrm{I}(z^*)$ is a holomorphic function in the whole complex plane z^* outside the cut (b, a). Using the following variable transformations:

$$z^*=\frac{a+b}{2}+\frac{a-b}{2}\zeta, \quad t=\frac{a+b}{2}+\frac{a-b}{2}\xi \quad (17)$$

the function $\mathrm{I}(z^*)$ can be represented as:

$$\mathrm{I}(z^*)=\frac{1}{\pi}\int_{-1}^{+1}\frac{b_x+ib_y}{\varsigma-\xi}d\xi \quad (18)$$

Let us assume that dislocation density can be expanded as a series of the first Chebyshev polynomial

$$b_x+ib_y=\frac{1}{\sqrt{1-\xi^2}}\sum_{m=0}^{\infty}\alpha_m T_m(\xi) \quad (19)$$

where $T_m(\xi)$ is the first polynomial of Chebyshev

$$T_m(\xi)=\cos(m\theta), \qquad \xi=\cos\theta\,.$$

Components b_x and b_y of the dislocation density have the square-root singularity $r^{-1/2}$ at crack tips. The first term of the right-hand side of Eq. (19) characterizes the desired singularity at the crack tips.

In order to get a closed analytical solution of Eq. (18), the series of the first Chebyshev polynomial is introduced in Eq. (19).

The opening displacement on the crack surface can be expressed by /5/ as:

$$\delta_x+\delta_y=-\int_b^t(bx+iby)dt=-\int_{-1}^{\xi}\frac{1}{\sqrt{1-\xi^2}}\sum_{m=0}^{\infty}\alpha_m T(\xi)d\xi.a_0$$
$$=a_0\alpha_0(\pi-\theta)+a_0\sum_{m=1}^{\infty}\alpha_m\frac{\sin(m\theta)}{m} \quad (20)$$

where $2a_0$ is crack length, c is distance from centre of crack to the interface (Fig. 2), we it is here:

$a_0=(a-b)/2;\ c=(a+b)/2;\ \xi=\cos(\theta)=(t-c)a_0.$

Opening displacement at point A should be zero, what is possible when $t=a;\ \xi=1;\ \theta=0$; producing $a_0=0$.

NUMERICAL SIMULATION OF CRACKS IN BIMATERIAL PLATES

Interfacial central crack between two dissimilar homogenous materials

To study the evolution of energy restitution rate for the case of interfacial crack in bimaterial plates, a specimen of ceramic/metal joint between Si_3N_4 (silicon nitride) and S45C steel was used. The silver based brazing alloy was the bonding between Si_3N_4 ceramic and S45C steel, /2/, Fig. 3.

The FEM is applied for the resolution of the interface problem using 8 nodes quadratic finite element meshing. The procedure *G*-théta available in code CASTEM, /13/, is used for evaluation of parameter *G*.

To compare our results to those obtained by Yijun J. Liu and Nan Xu, /2/, we have evaluated G parameter using the following equations:

$$G=\frac{1}{2}(1-\beta^2)\left[\frac{1-\nu_1^2}{E_1}+\frac{1-\nu_2^2}{E_2}\right]|K|^2 \quad (21)$$

where

$$\beta=\frac{1}{2}\frac{\mu_1(1-2\nu_2)-\mu_2(1-2\nu_1)}{\mu_1(1-\nu_2)+\mu_2(1-\nu_1)} \quad (22)$$

$$|K|=\sqrt{K_I^2+K_{II}^2} \quad (23)$$

where m_1, m_2 represent shear modulus of the materials, and K_I, K_{II} are stress intensity factors relative to fracture modes I and II, respectively.

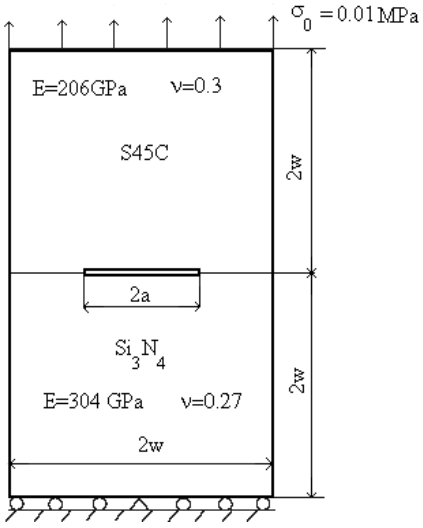

Figure 3. Bimaterial plate containing a crack at the interface subjected to an uniform tensile load.
Slika 3. Bimaterijalna ploča sa prslinom na interfejsu izložena ravnomernom zateznom opterećenju

Due to the vertical symmetry of specimens, only half of the cracked plate is considered in the modelization by 8 nodes quadratic finite elements, as shown in Fig. 4.

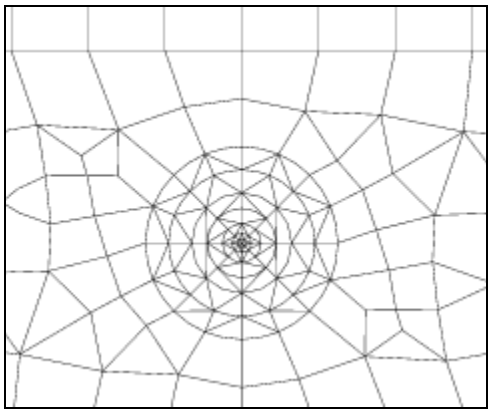

Figure 4. Finite elements meshing of the interfacial crack tip in bimaterial plate.
Slika 4. Mreža konačnih elemenata oko vrha prsline na interfejsu bimaterijalne ploče

The values of released energy rate are given in Fig. 5. Numerical results are in a good agreement with the results of /14/ and /2/, maximum difference is less than 5%.

Cracks normal to the interface in bimaterial plates

In this application, bimaterial specimens of aluminium and PSM-1, of elastic constants given in Table 1, with a crack (W = L = 15 mm, t = 5.5 mm), are considered (Fig. 6) for different crack lengths corresponding to crack ratios (a/W = 0.1, 0.2, 0.3, 0.4, 0.5, 0.6, 0.7, 0.8, 0.9, 0.99), /7/.

Table 1. Elastic constants of the materials.
Tabela 1. Elastične konstante materijala

	Young modulus E (MPa)	Poisson ratio ν
Aluminium	64300	0.33
PSM-1	3050	0.39

Specimens have been obtained by joining two aluminium thin plates and a plate made of PSM-1 polycarbonate with liquid Araldite D adhesive, /7/.

The specimens are subjected to tensile force F = 6600 N, that produced a stress field at the upper and lower edges of the plate as shown in Fig. 7.

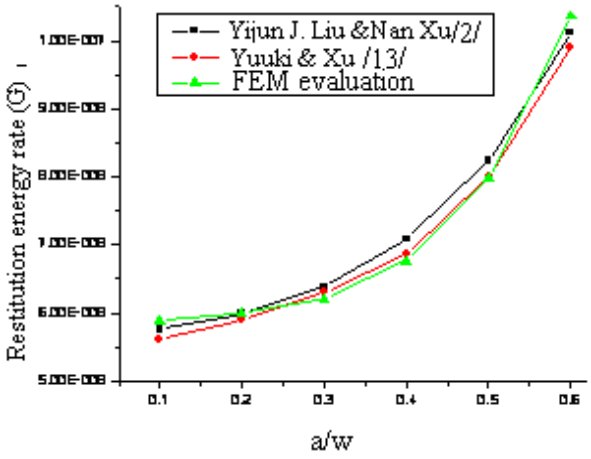

Figure 5. Numerical results by FEM calculation of G parameters vs. crack ratio a/W in an approximate evaluation from /14/ and /2/.
Slika 5. Numerički rezultati proračuna MKE zavisnosti G parametra od odnosa prsline a/W u približnoj oceni iz Ref. /14/ i /2/

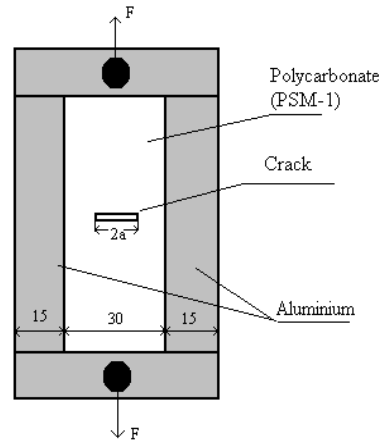

Figure 6. Geometry of the cracked specimen subjected to tensile loading, /7/.
Slika 6. Geometrija epruvete sa prslinom izložene zateznom opterećenju, /7/

Due to the symmetry according to both axes x, y of reference, only the quarter of plate is considered in the modelization of the specimen as shown in Fig. 7.

Applied finite elements meshing near the crack with 8 nodes quadratic finite elements is shown in Fig. 8.

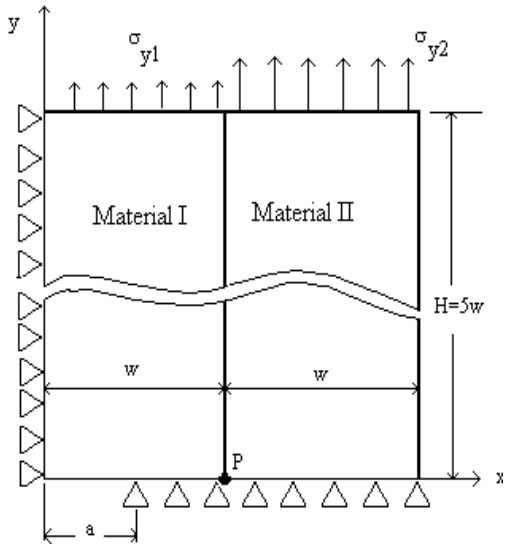

Figure 7. Modelization of bimaterial plate.
Slika 7. Model bimaterijalne ploče

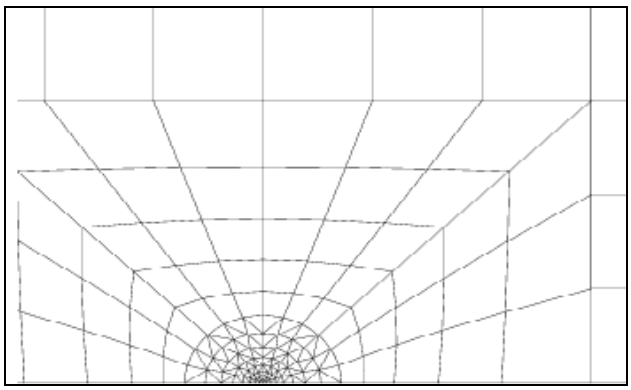

Figure 8. FEM meshing of bimaterial plate near the crack tip.
Slika 8. Mreža KE za bimaterijalnu ploču u blizini vrha prsline

Figure 9 shows results of stress intensity factors calculated by FEM and those reported in Ref. /7/ using Red Green Blue (RGB photoelasticity) experiments, /15/, and a semi-analytic relationship defined as:

$$\bar{K}_I = 1 - \frac{\lambda_1(\alpha_D - \beta_D\lambda_1)}{2\alpha_D}\tan\left[\frac{\pi}{2}\lambda_1(\alpha_D + \beta_D\lambda_1)\left(\frac{a}{w}\right)^{\alpha_D+\beta_D\lambda_1}\right] \quad (24)$$

where α_D and β_D are two Dundur's parameters and λ_1 is the order of singularity.

Values of normalised stress intensity factor obtained numerically by FEM are in a good agreement with the ones evaluated in /7/ by Red, Green, Blue (RGB) experimental photoelasticity and Eq. (24).

In Fig. 9, the presence of the crack in the less stiffened material and the effect of interface materials mismatch produced a "closing" bridging stress intensity factor that decreases the stress intensity factor resulting from external load with the crack length, i.e. when the crack tip is close to the interface.

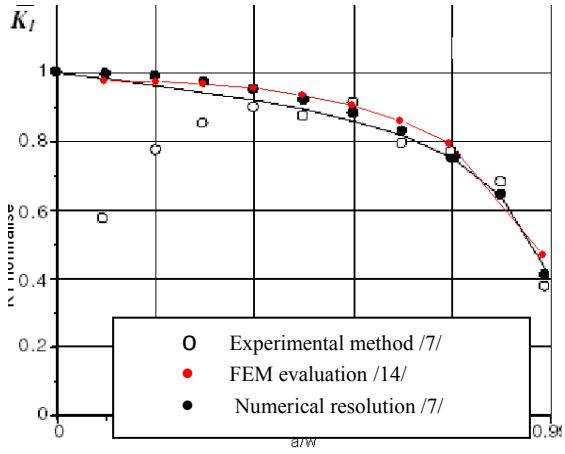

Figure 9. Evaluation by FEM of normalised stress intensity factor ($\bar{K}_I = K_I/\sigma_y\sqrt{\pi a}$) vs crack length ratio (a/W).

Slika 9. Ocena pomoću MKE zavisnosti normalizovanog faktora intenziteta napon ($\bar{K}_I = K_I/\sigma_y\sqrt{\pi a}$) i odnosa dužine prsline (a/W)

The numerical simulation in Fig. 10 shows the decreased tendency of normalised stress intensity factors when crack propagates in the domain of material I (PSM-1, Table 1). The evaluation has been considered also when the crack propagates in the more stiffened domain of the bimaterial plate (Aluminium, Table 1). In this case the normalised stress intensity factor increases with ratio a/W.

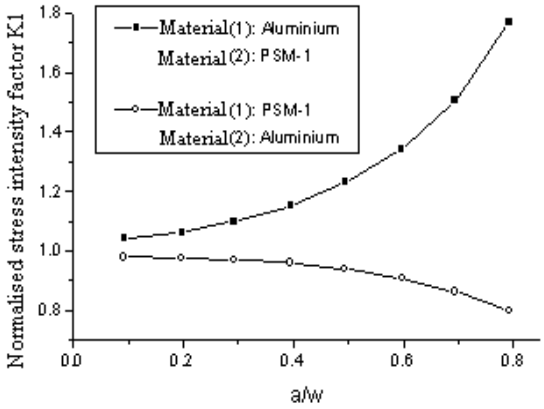

Figure 10. Evaluation of the normalised stress intensity factor with the crack propagation and material properties

Slika 10. Zavisnost normalizovanog faktora intenziteta napona od rasta prsline i osobina materijala

It is important to note that the ratio of evolution of $\bar{K}_I$ parameter in Fig. 10 will be more significant when the geometric crack ratio is greater than $a/W = 0.4$; it means that when the crack tip is close to the interface.

Cracks parallel to the interface

In the next simulation, an attempt is made to show the effect of lateral position of crack on the release energy rate G when the crack is located at a distance h from the interface. The evolution of parameter G is plotted in Fig. 11.

Results presented in Fig. 11 show that G parameter increases when the crack is too far from the interface. The evolution depends on the material elastic constants in the domain containing the crack and crack ratio a/W. For the same geometry crack ratio a/W, greater G values are noted when the crack is positioned in the material of the minor value of Young modulus ($E = 206$ GPa, $\nu = 0.30$).

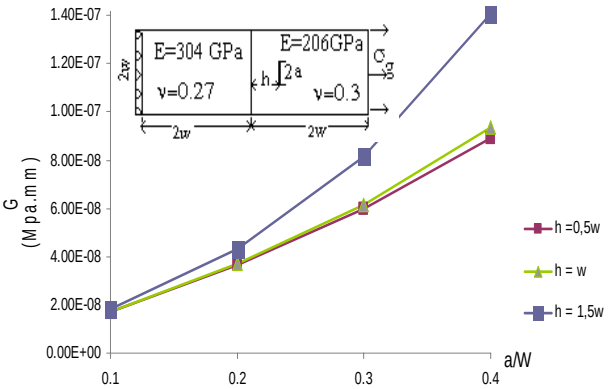

a) Crack in aluminium

a) Prslina u aluminijumu

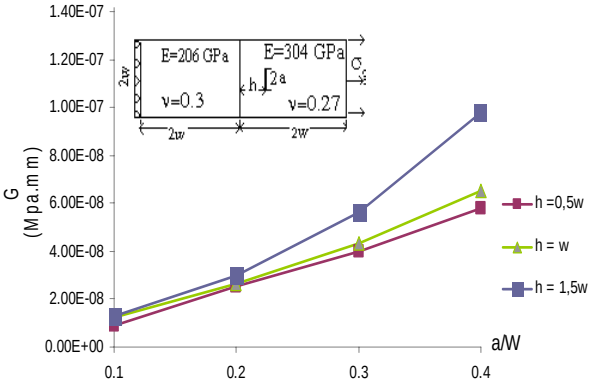

b) Crack in PSM-1 material

b) Prslina u PSM-1 materijalu

Figure 11. Evolution of the released energy rate G with the lateral position h of the crack

Slika 11. Zavisnost od brzine oslobađanja energije G od bočnog položaja h prsline

Interface cracks in mixed mode fracture

This section concerns the effect of mixed mode and mechanical properties of the bimaterial on fracture parameters, especially on the released energy rate G.

The specimen of bimaterial plate contained an inclined edge crack of various ratio (a/W = 0.1, 0.2, 0.3, 0.4, 0.5, 0.6) and inclination angles. The cracked plate is subjected to a tensile loading stress σ_g = 1 MPa, Fig. 12. The problem has been solved in plane stress condition by using the finite element method for specimen modelization (Fig. 13).

After numerical resolution in term of G_{eq}, according to

$$G_{eq} = \sqrt{G_I^2 + G_{II}^2} \tag{25}$$

Released energy rate values are plotted in Fig. 14 for several crack orientations in aluminium and the PSM–1 material. Obtained results show that the released energy rate G increases with crack length a for cracks positioned in both materials.

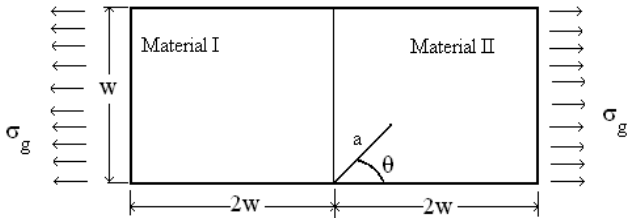

Figure 12. Inclined edge crack in bimaterial plate.
Slika 12. Nagnuta prslina u bimaterijalnoj ploči

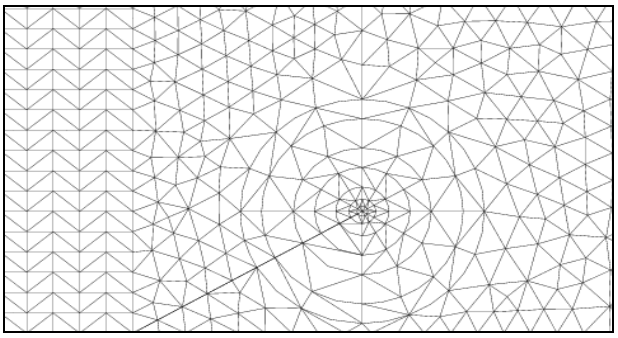

Figure 13. Finite element modelling of interface crack near the tip.
Slika 13. Model konačnih elemenata prsline na interfejsu oko vrha

Graphs of G_{eq} in Fig. 14 show that this parameter increases with crack length. It is important to note that when the crack propagation is located in the domain of more stiff material of specimen (aluminium, Table 1), the values of released energy rate G_{eq} decreased (Fig. 14b) for all studied inclinations of crack angle.

CONCLUSIONS

In this paper, the stress field near the crack tip has been studied for several orientations and positions of crack by means of numerical analysis. The singularity of the stress and its complexity for cracks along the interface was considered by evaluating energy release rate G.

The results for G parameter for a central interfacial crack shown in Fig. 5 are in a good agreement with those obtained, presented in Ref. /14/. This fracture parameter increases with crack length a. This tendency of G has the same evolution as in the case when the crack is in a homogenous media. The elastic mismatch has a significant effect on the values of the released energy rate G.

When the crack is perpendicular to the interface, the decreased curve of normalised stress intensity factor $\bar{K}_I$ obtained by A. Cirello and B. Zuccarello in Ref. /7/ is confirmed for all geometric crack ratios a/W (Fig. 9). This tendency of stress intensity factor decrease is explained in /7/ by the significant presence of "bridging effect". The graphs plotted in Fig. 10 show that the influence of the "bridging effect" is negligible when the crack propagates in the aluminium domain, i.e. the normalised stress intensity factor increases with crack length.

For the inclined edge crack emanating from the interface, results in Fig. 14 show that G parameter increases with crack inclination angle; this tendency is more significant for ratio $a/W \geq 0.4$ and for inclination angle $\theta = 60°$. The elastic mismatch effect on the energy release rate is more important when the crack tip orientation is closed to the interface. As mentioned above, the elastic constants of the domain containing the crack have the same effect on the G parameter.

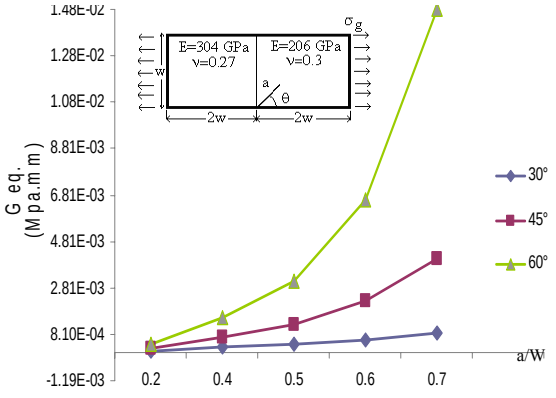

a) Crack in aluminium
a) Prslina u aluminijumu

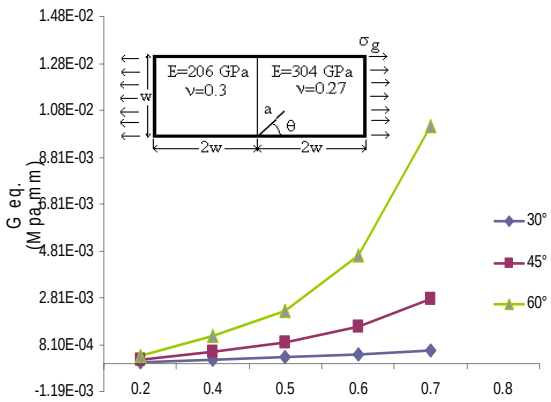

b) Crack in PSM–1 material
b) Prslina u PSM–1 materijalu

Figure 14. Evolution of released energy rate G_{eq} with crack inclination angle and ratio a/W.
Slika 14. Zavisnost brzine oslobađanja energije G_{eq} od ugla nagiba i odnosa a/W

REFERENCES

1. Marur, P.R., Tippur, H.V., *A strain gage method for determination of fracture parameters in bimaterial systems*, Eng. Frac. Mech, No. 64 (1999), 87-104.
2. Liu, Y.J., Nan, Xu., *Modeling of interface cracks in fiber-reinforced composites with the presence of interphases using the boundary element method*, Mechanics of Materials, Vol. 32, Issue 12 (2000), 769-783.
3. Shi, J.P., *Stress intensity factors for interface crack in finite size specimen using a generalised variational approach*, Theoretical and Applied Fracture Mechanics 28 (1998), 223-230.
4. Bjerken, Ch., Persson, Ch, *A numerical method for calculating stress intensity factors for interface cracks in bimaterials*, Eng. Frac. Mech 68 (2001), 235-246.
5. Wang, T.C., Stahle, P., *Stress state in front of a crack perpendicular to bimaterial interface*, Eng. Frac. Mech, Vol. 59, No. 4 (1998), 471-485.
6. Kang Yilan, Lu Hua, *Investigation of near-tip displacement fields of a crack normal to and terminating at a bimaterial interface under mixed-mode loading*, Eng. Frac. Mech 69 (2002), 2199–2208.
7. Cirello, A., Zuccarello, B., *On the effects of a crack propagating toward the interface of a bimaterial system*, Eng. Frac. Mech (2006), 1264-1277.
8. Nao Aki Noda, Takao Kouyane, Yositomo Kinoshita, *Stress intensity factors of an inclined elliptical crack near a bimaterial interface*, Eng. Fract. Mech. 73 (2006), 1292-1320.
9. Rice, J.R., Suo, Z., Wang, J.S., *Mechanics and thermodynamics of brittle interfacial failure in bimaterial systems*, Metal-Ceramic Interfaces, M. Ruhle, A.G. Evans, M.F. Ashby and J.P. Hirth Eds., Pergamon Press, New York 1990, 269-294.
10. Dundur, J., *Edge-bonded dissimilar orthogonal elastic wedges*, J. of Appl. Mech. 36 (1969), 650.
11. Malyshev, B.M., Salganik, R.L., *The strength of adhesive joints using the theory of cracks*, Int. J. Fract Mech., 5 (1965), 114-28.
12. Suo, Z., *Singularities interacting with interface and cracks*, Journ. of Solids and Structures, 25 (1989), 1133-1142.
13. Yuuki, R., Xu, J.Q., *Boundary element method and its applications to the analyses of dissimilar materials and interface cracks*, Computational and Experimental Fracture Mechanics: Developments in Japan, Computational Mechanics Publications, Southampton, UK (1994), 61-90.
14. Code CASTEM (2000), Commissariat à l'Energie Atomique CEA-DEN/DMSS/SEMT.
15. Ajovalasit, A., Barone, S., Petrucci, G., *Toward RGB photoelasticity—full field photoelasticity in white light*, Exp Mech, 35 (1995), 193-200.

Faculty of Technology and Metallurgy, University of Belgrade
Faculty of Mechanical Engineering, University of Belgrade
Society for Structural Integrity and Life
and
Laboratoire de Fiabilité Mécanique de l'Ecole Nationale d'Ingénieurs de Metz
under the auspice of European Structural Integrity Society

organize

NT2F9

Ninth International Conference

New Trends in

FATIGUE and FRACTURE

"Failures of materials and structures by fatigue and fracture"

October 12–14, 2009